01 - Introduction SPO

02 - Orientation and Preferred Orientation

03 - Passive active deformation implications on Shape Preferred Orientation

04 - 2D Shape Preferred Orientation 1) of classified images

05 - 2D Shape Preferred Orientation 2) of greyscale images

06 - 3D Shape Preferred Orientation

UNIVERSITÉ DE NANTES
FACULTÉ DES SCIENCES ET TECHNIQUES

Pr. Patrick Launeau
patrick.launeau@univ-nantes.fr

When each grain of material undergoes the same deformation without any viscosity contrast, the deformation is said to be passive

Warning
(X,Y) arbitrary
2D section

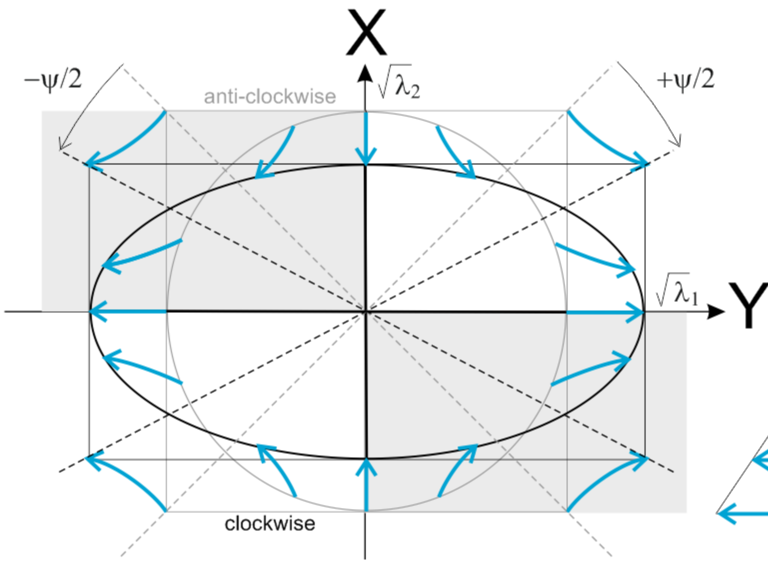

Pure shear

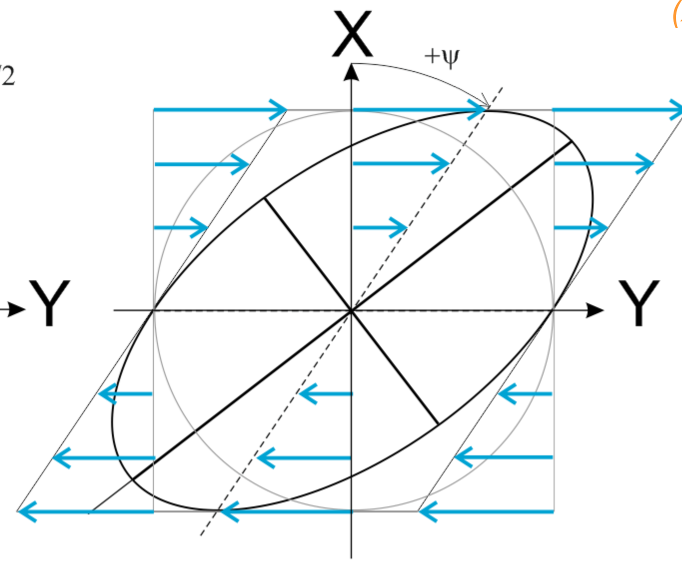

Simple shear

The pure shear is a coaxial deformation with 50% dextral and 50% sinistral flux of material (blue arrows) while simple shear is not coaxial and display 100% dextral (clockwise) or sinistral (anticlockwise) material flux (dextral in the present figure).

In case of iso-surface pure shear deformation, the shape ratio of the ellipse of deformation is equal the quadratic elongation λ and its shortening is equal to the inverse of the elongation

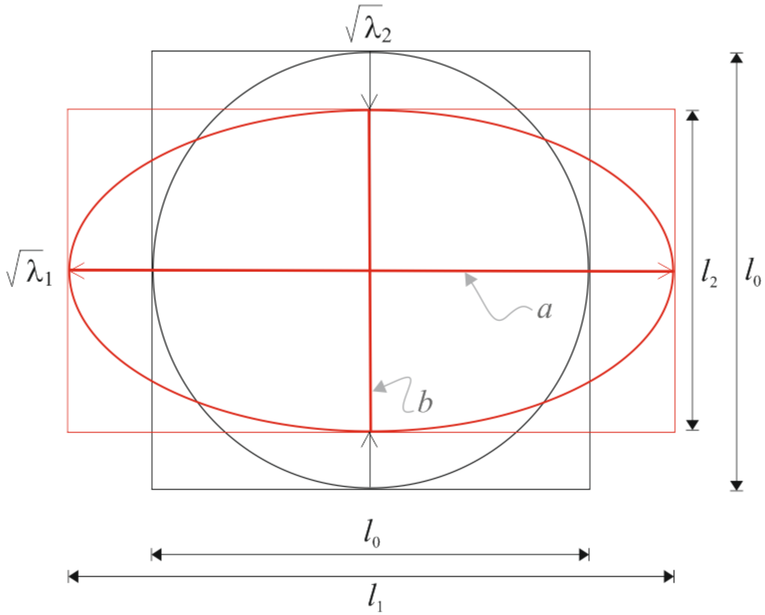

$$R = a/b$$

$$a = l_1/l_0 = \sqrt{\lambda_1}$$

$$b = l_2/l_0 = \sqrt{\lambda_2}$$

$$\sqrt{\lambda_1} \cdot \sqrt{\lambda_2} = 1$$ Iso-surface condition

$$\sqrt{\lambda_2} = 1/\sqrt{\lambda_1}$$

$$R = \lambda_1$$

Normalization to an unitary surface: $a_n = l_1/\sqrt{\lambda_1 \cdot \lambda_2}$

The shape ratio is also proportional to ω the angle of invariant radius during the deformation

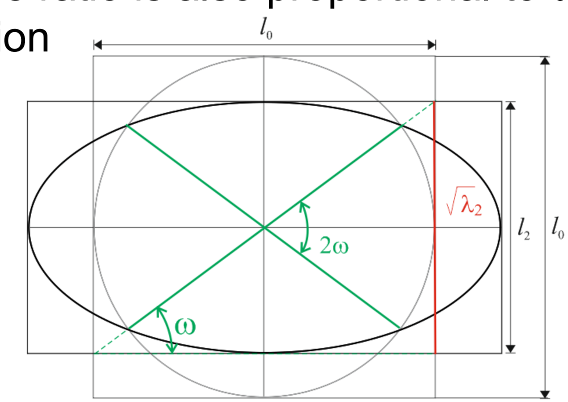

$$l_2/l_0 = \sqrt{\lambda_2} = \tan\omega = 1/\sqrt{\lambda_1}$$

$$R = \sqrt{\lambda_1}/\sqrt{\lambda_2} = 1/(\tan\omega)^2$$

The shape ratio of an ellipse deformed by simple shear is proportional to the shear angle ψ usually converted in simple shear rate γ as it follows

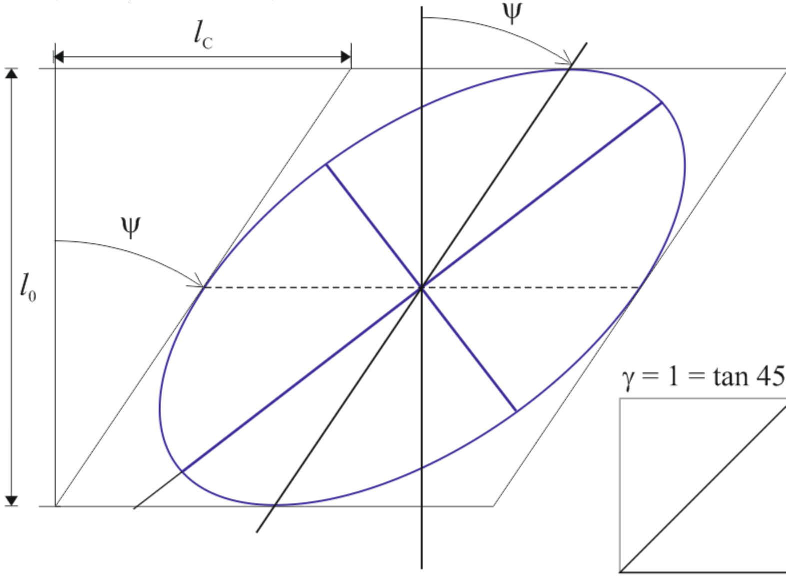

$$\gamma = l_c / l_0 = \tan\psi$$

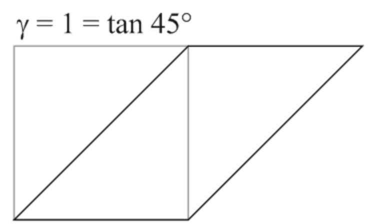

The shape ratio of the ellipse of deformation is also proportional to ω and can be estimated as it follows

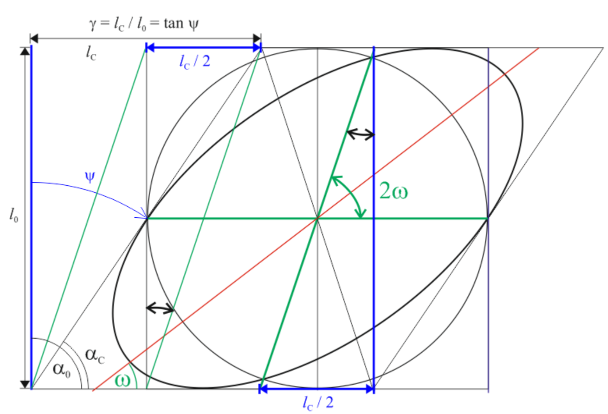

$$\cot\alpha_c = \cot\alpha_0 + \gamma$$

$$0.5 \cdot l_c / l_0 = \gamma / 2 = (\tan\psi)/2 = \cot(2\cdot\omega) = 1/\tan(2\cdot\omega)$$

$$\gamma = 2/\tan(2\cdot\omega)$$

$$\omega = 0.5 \cdot \arctan(2/\gamma)$$

$$R = 1/(\tan\omega)^2$$

So a simple shear can be decomposed in a rotation and an elongation

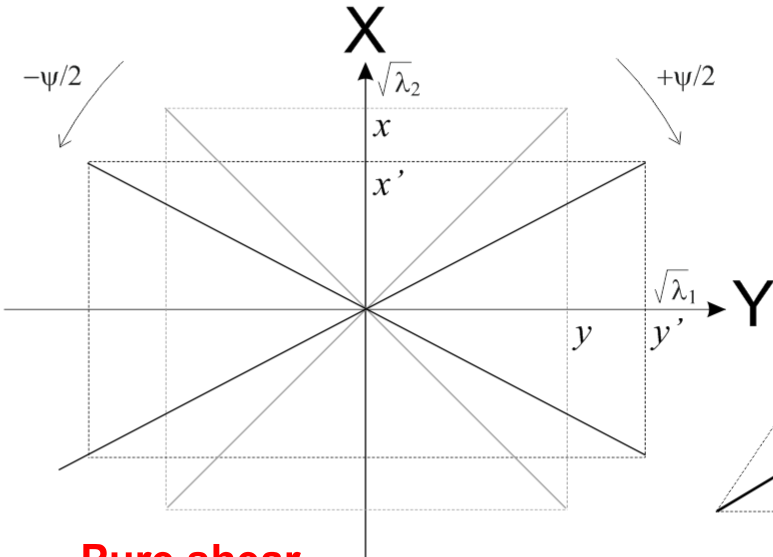

Pure shear

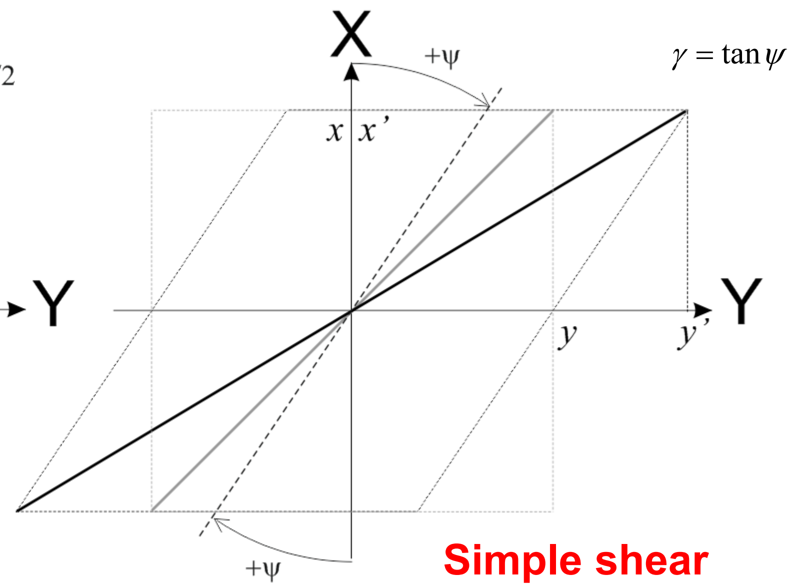

Simple shear

$$x' = \sqrt{\lambda_2} \cdot y$$
$$y' = \sqrt{\lambda_1} \cdot y$$

$$\begin{vmatrix} x' \\ y' \end{vmatrix} = \begin{vmatrix} \sqrt{\lambda_2} & 0 \\ 0 & \sqrt{\lambda_1} \end{vmatrix} \times \begin{vmatrix} x \\ y \end{vmatrix}$$

$$x' = x$$
$$y' = \gamma \cdot x + y$$

$$\begin{vmatrix} x' \\ y' \end{vmatrix} = \begin{vmatrix} 1 & 0 \\ \gamma & 1 \end{vmatrix} \times \begin{vmatrix} x \\ y \end{vmatrix}$$

2D simulations on the (X,Y) section of a pure shear, a simple shear and a combination of both shear applied towards the [Y] direction. The simple shear rotation ψ twist the axis [X] which causes a non-coaxial deformation characterized by an asymmetric matrix of deformation.

$$\boxed{\mathbf{V'} = \quad \mathbf{M} \quad \mathbf{V}}$$

$$\begin{vmatrix} x' \\ y' \end{vmatrix} = \begin{vmatrix} \sqrt{\lambda_2} & 0 \\ \gamma & \sqrt{\lambda_1} \end{vmatrix} \times \begin{vmatrix} x \\ y \end{vmatrix}$$

Combination of pure and simple shear

Warning
(X,Y) arbitrary
2D section

Let now consider 2 vectors with an initial length l and a final one l'

$$x = l \cdot \cos\psi$$
$$y = l \cdot \sin\psi$$

and simulate a deformation

$$\boxed{V' = \mathbf{M} \quad V}$$

$$\begin{vmatrix} x' \\ y' \end{vmatrix} = \begin{vmatrix} \sqrt{\lambda_2} & 0 \\ \gamma & \sqrt{\lambda_1} \end{vmatrix} \times \begin{vmatrix} x \\ y \end{vmatrix}$$

$$x' = l' \cdot \cos\psi'$$
$$y' = l' \cdot \sin\psi'$$

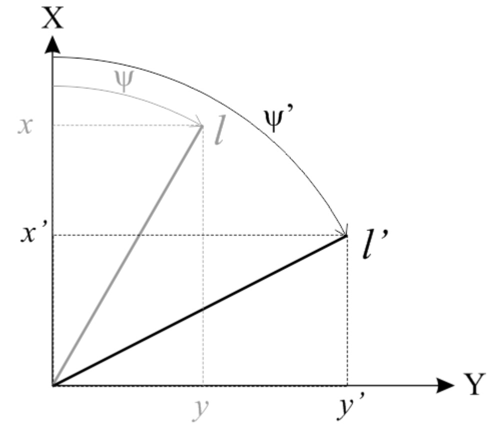

Warning (X,Y) arbitrary 2D section

It is possible to retrieve the deformation rate by using the cosine directions as seen in PO chapter. But this method only considers the rotation between initial and final stage

$$\varphi' = \arctan\left(\frac{y'}{x'}\right)$$

$$V' = R\ V$$

Warning
(X,Y) arbitrary
2D section

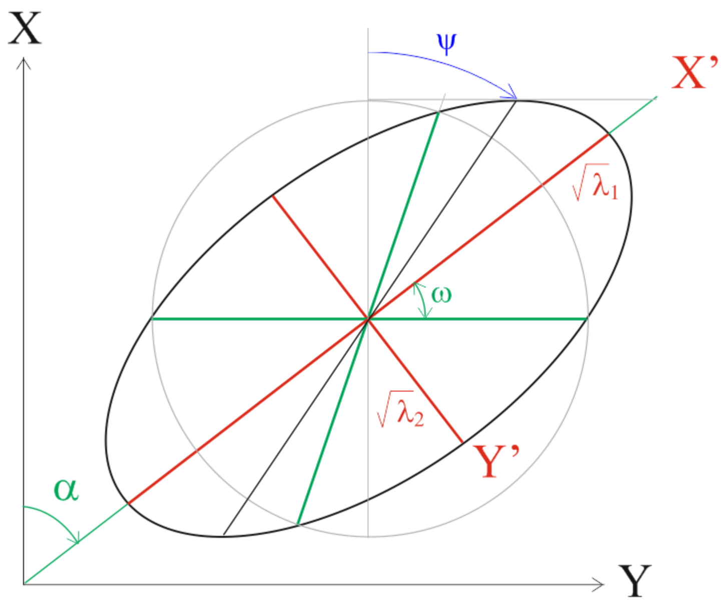

$$\mathbf{V'} = \mathbf{M}\,\mathbf{V}$$

$$\mathbf{R}\,\mathbf{V'} = \mathbf{M}\,\mathbf{R}\,\mathbf{V}$$

$$\mathbf{R}^{-1}\,\mathbf{R}\,\mathbf{V'} = \mathbf{R}^{-1}\,\mathbf{M}\,\mathbf{R}\,\mathbf{V}$$

$$\mathbf{V'} = \mathbf{R}^{-1}\,\mathbf{M}\,\mathbf{R}\,\mathbf{V}$$

$$\mathbf{\Lambda} = \mathbf{R}^{-1}\,\mathbf{M}\,\mathbf{R}$$

There is no easy determination of deformations including non coaxial simple shear component forming asymmetric matrix **M**. If **V** is one of the vectors forming the initial ellipse, **V'** is the final ellipse in which X and Y loose their perpendicularity. A simplification of the problem consists in the determination of a rotation **R** from initial XY to the final X'Y' orthonormal coordinate system of the new ellipse. Afterward, a back rotation **R'** reorient the final vectors in the initial XY coordinate system. This rotation α gives access to the eigenvectors **R** diagonalizing **M** in a matrix of eigenvalues **Λ** giving the intensity of an equivalent pure shear.

Thus, a combination of pure and simple shear is decomposed in one rotation and one pure shear.

The detection of a simple shear component required on external reference such as a marker of the shear plane

Warning (X,Y,Z) is the image coordinate system which should not be confused with (A,B,C) the ellipsoid deformation coordinate system

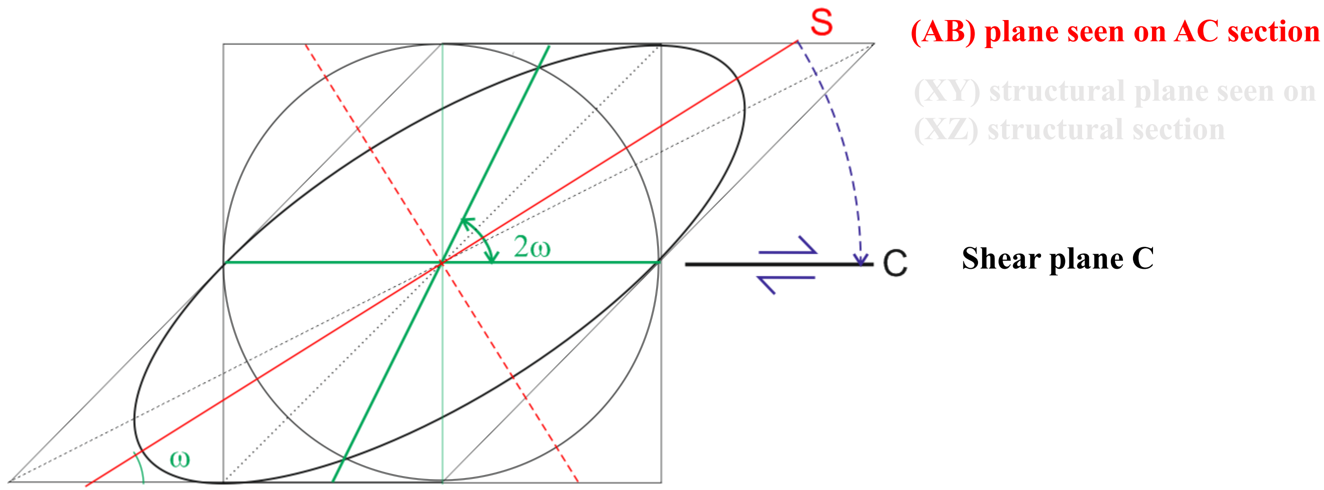

The plane of schistosity S corresponds to the structural (X,Y) plane noted (A,B) in the convention of this course. The angle measured between the S (A,B) plane and the shear plane C on a section (A,C) is equal to the characteristic angle ω. It ranges from 45° with the first shearing deformation increment to 0° for an infinite deformation.

Let now simulates an ellipse with the calculation of their radius l and test the vector distribution matrix around their gravity centers x_c, y_c

$$x_c = \frac{1}{N}\sum_i (x_i)$$

$$y_c = \frac{1}{N}\sum_i (y_i)$$

Radius of an ellipse

$$x_\psi = l_\psi \cdot \cos(\alpha+\psi) \qquad y_\psi = l_\psi \cdot \sin(\alpha+\psi)$$

with

$$\frac{1}{l_\psi^2} = \frac{1}{l_{ellipse\,\psi}^2} = \frac{\cos^2\psi}{a^2} + \frac{\sin^2\psi}{b^2}$$

$$l_{oval\,\psi}^2 = a^2 \cdot \cos^2\psi + b^2 \cdot \sin^2\psi$$ would draw an oval

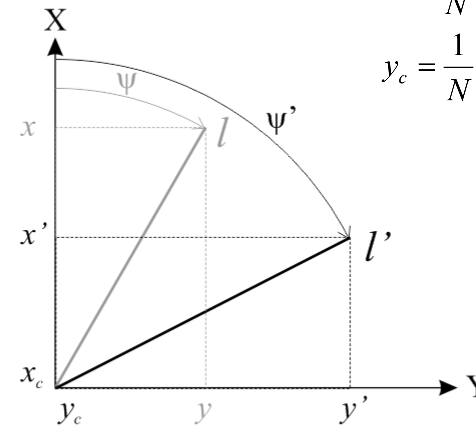

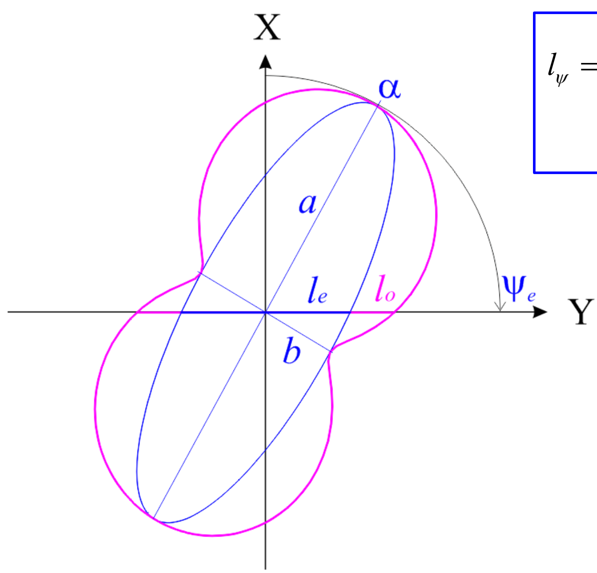

$$l_\psi = \frac{1}{\sqrt{\dfrac{\cos^2\psi}{a^2} + \dfrac{\sin^2\psi}{b^2}}}$$

$$m_{xx} = \frac{1}{N}\sum_i (x_i - x_c)^2$$

$$\mathbf{M} = \begin{vmatrix} m_{xx} & m_{xy} \\ m_{xy} & m_{yy} \end{vmatrix} \qquad m_{xy} = \frac{1}{N}\sum_i (x_i - x_c)(y_i - y_c)$$

$$m_{yy} = \frac{1}{N}\sum_i (y_i - y_c)^2$$

The main eigenvector of $\mathbf{M}$ effectively retrieves the ellipse orientation α and their eigenvalues ratio is equal to its shape ratio R

$$R = \sqrt{\frac{\mu_1}{\mu_2}}$$

The exact size of the ellipse is given by:

$$a = \sqrt{2\mu_1}$$

$$b = \sqrt{2\mu_2}$$

Shape **Preferred Orientation (OCW-UN-SPO) Launeau P. 2017**

The drawing of an ellipse with a regular step of 10° gives case 1 plot. $\alpha_{sampling} = 10°$ starting from the orientation α of a

In case 2, the drawing of an ellipse with a step proportional to its elongation direction α is required for the true simulation of an ellipse $\alpha_{sampling} = \arctan\left(\frac{R\sin\alpha_{step}}{\cos\alpha_{step}}\right)$

All the radius of an initial disk undergoing a deformation converge towards α its main direction of elongation a.

This will be an important property for the following image analyses which tend to explore the images with constant angular step.

The shape ratio of the ellipse is 3 and we found:

	Case 1		Case 1	Case 2	
R_{Lc}	2.978	R	1,726	2.983	3
a_{Lc}	1.604	a	1.221	1.727	1.732
b_{Lc}	0.539	b	0.807	0.579	0.577

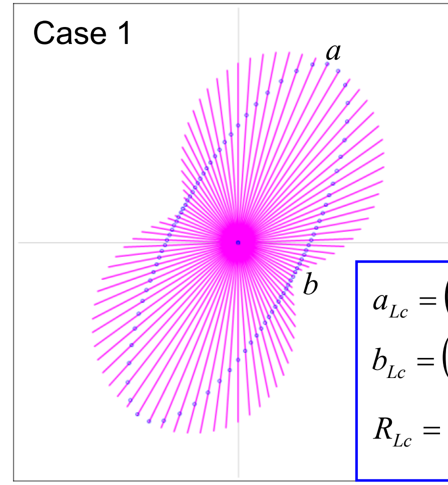

$$Rf = \frac{\mu_1}{\mu_2}$$

$$a_{Lc} = \left(2\mu_1^{1,5}/\mu_2^{0,5}\right)^{0,5}$$

$$b_{Lc} = \left(2\mu_2^{1,5}/\mu_1^{0,5}\right)^{0,5}$$

$$R_{Lc} = \frac{a_{Lc}}{b_{Lc}} = \sqrt{\frac{\mu_1}{\mu_2}}$$

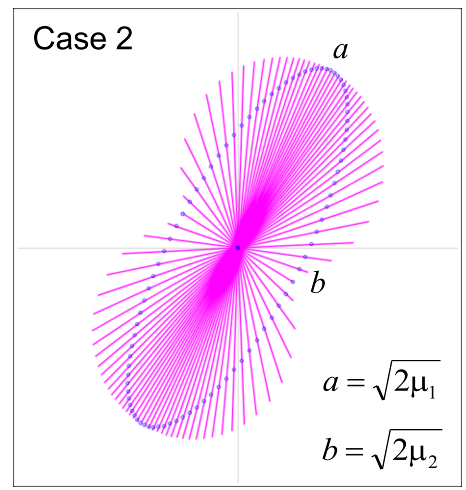

$$R = \sqrt{\frac{\mu_1}{\mu_2}}$$

The analysis with a constant angular step misses the rotation due to the deformation similarly to the cosine direction which misses the vector elongation. In such cases the true shape ratio is given by Rf (eigenvalue ratio) instead of R (eigenvalue ratio square root). Alternatively the ratio of the weighted sizes a_{Lc} and b_{Lc} can be used to calculate R.

Launeau (2004)

$$x_c = \frac{1}{N}\sum_i (x_i)$$
$$y_c = \frac{1}{N}\sum_i (y_i)$$

Further simulations can be done with various shape weighting:

Cosine directions of J angles

weight = 1

$$m_{xx} = \frac{1}{J}\sum_j \cos(\alpha_j)^2$$
$$m_{yx} = m_{xy} = \frac{1}{J}\sum_j \cos(\alpha_j)\sin(\alpha_j)$$
$$m_{yy} = \frac{1}{J}\sum_j \sin(\alpha_j)^2$$

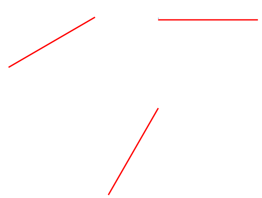

$$\mathbf{M} = \begin{vmatrix} m_{xx} & m_{xy} \\ m_{yx} & m_{yy} \end{vmatrix}$$

$$\begin{bmatrix} \sqrt{Rf} & 0 \\ 0 & 1/\sqrt{Rf} \end{bmatrix} = \mathbf{R}^{-1}\cdot\mathbf{M}\cdot\mathbf{R}$$

Harvey & Laxtion (1980)

Vector lengths of J lines

weight = l_j

$$m_{xx} = \frac{1}{J}\sum_j (x_j - x_c)^2$$
$$m_{xy} = \frac{1}{J}\sum_j (x_j - x_c)(y_j - y_c)$$
$$m_{yy} = \frac{1}{J}\sum_j (y_j - y_c)^2$$

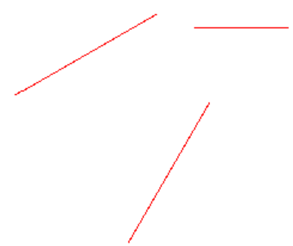

$$\mathbf{M} = \begin{vmatrix} m_{xx} & m_{xy} \\ m_{yx} & m_{yy} \end{vmatrix}$$

$$\begin{bmatrix} a^2/2 & 0 \\ 0 & b^2/2 \end{bmatrix} = \mathbf{R}^{-1}\cdot\mathbf{M}\cdot\mathbf{R}$$

Surface areas of J ellipses

weight = A_j

$$m_{xxj} = \frac{1}{A_j}\sum_{ij} (x_{ij} - x_{cj})^2$$
$$m_{xyj} = \frac{1}{A_j}\sum_{ij} (x_{ij} - x_{cj})(y_{ij} - y_{cj})$$
$$m_{yyj} = \frac{1}{A_j}\sum_{ij} (y_{ij} - y_{cj})^2$$

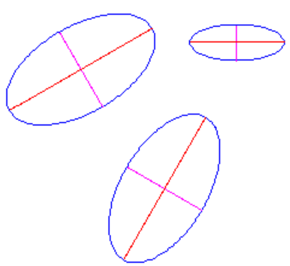

$$\mathbf{M} = \frac{1}{J}\sum_j \mathbf{M}_j = \frac{1}{J}\begin{vmatrix} \sum_j m_{xxj} & \sum_j m_{xyj} \\ \sum_j m_{xyj} & \sum_j m_{yyj} \end{vmatrix}$$

$$\begin{bmatrix} a^2/4 & 0 \\ 0 & b^2/4 \end{bmatrix} = \mathbf{R}^{-1}\cdot\mathbf{M}\cdot\mathbf{R}$$

Rink (1976)

The characterization of 3D ellipsoid is possible with Flinn and Jelinek parameters

Prolate → linear, elongated, constrictive deformation
Planolinear → simple shear, uniaxial pure shear
Oblate → planar, flattened, divergent deformation

Flinn diagram

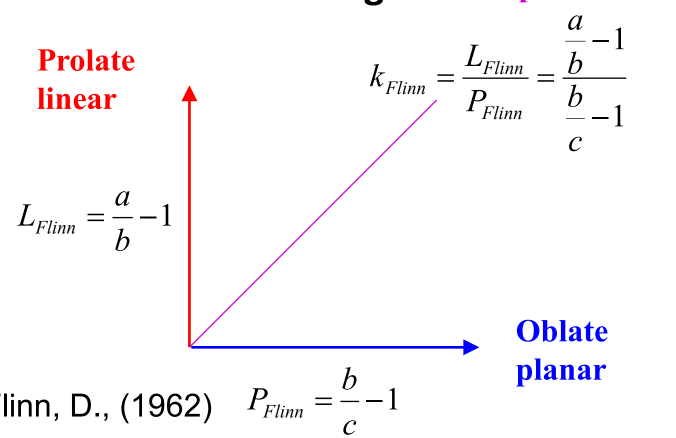

Flinn, D., (1962)

Let note Flinn the parameter k to avoid confusion with the shape parameter k

$Flinn = 0$	for	$a = b > c$		
$Flinn = 1$	for	$a > b > c$	with	$a / b = b / c$
$Flinn = \infty$	for	$a > b = c$		

Jelinek diagram

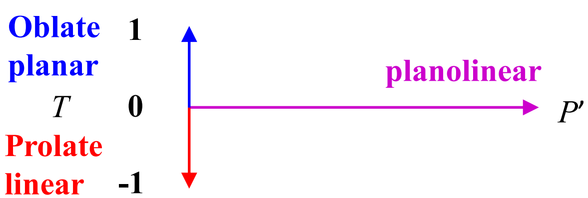

Jelinek, V., (1981)

Let the ellipsoid a, b, c be respectively b_1, b_2, b_3 :

$P' = \exp[2(l_1^2 + l_2^2 + l_3^2)]^{1/2}$, with $l_n = \ln(b_n/b_B)$ and $b_B = (b_1.b_2.b_3)/3$

$T = [2(\ln b_2 - \ln b_3)/(\ln b_1 - \ln b_3)] - 1$

$T = 1$	for	$a = b > c$		
$T = 0$	for	$a > b > c$	with	$a / b = b / c$
$T = -1$	for	$a > b = c$		

Jelinek's parameters varying from -1 to 1 are more often used in SPO and AMS studies than Flinn parameters varying from 0 to ∞

3D ellipsoid deformation with a constant volume $\lambda_1 \cdot \lambda_2 \cdot \lambda_3 = 1$ or $\sqrt{\lambda_1} \cdot \sqrt{\lambda_2} \cdot \sqrt{\lambda_3} = 1$ can displays surface area changes.
The 2D hypothesis of constant surface area is not valid in 3D for which compensations between sections maintain the volume constant

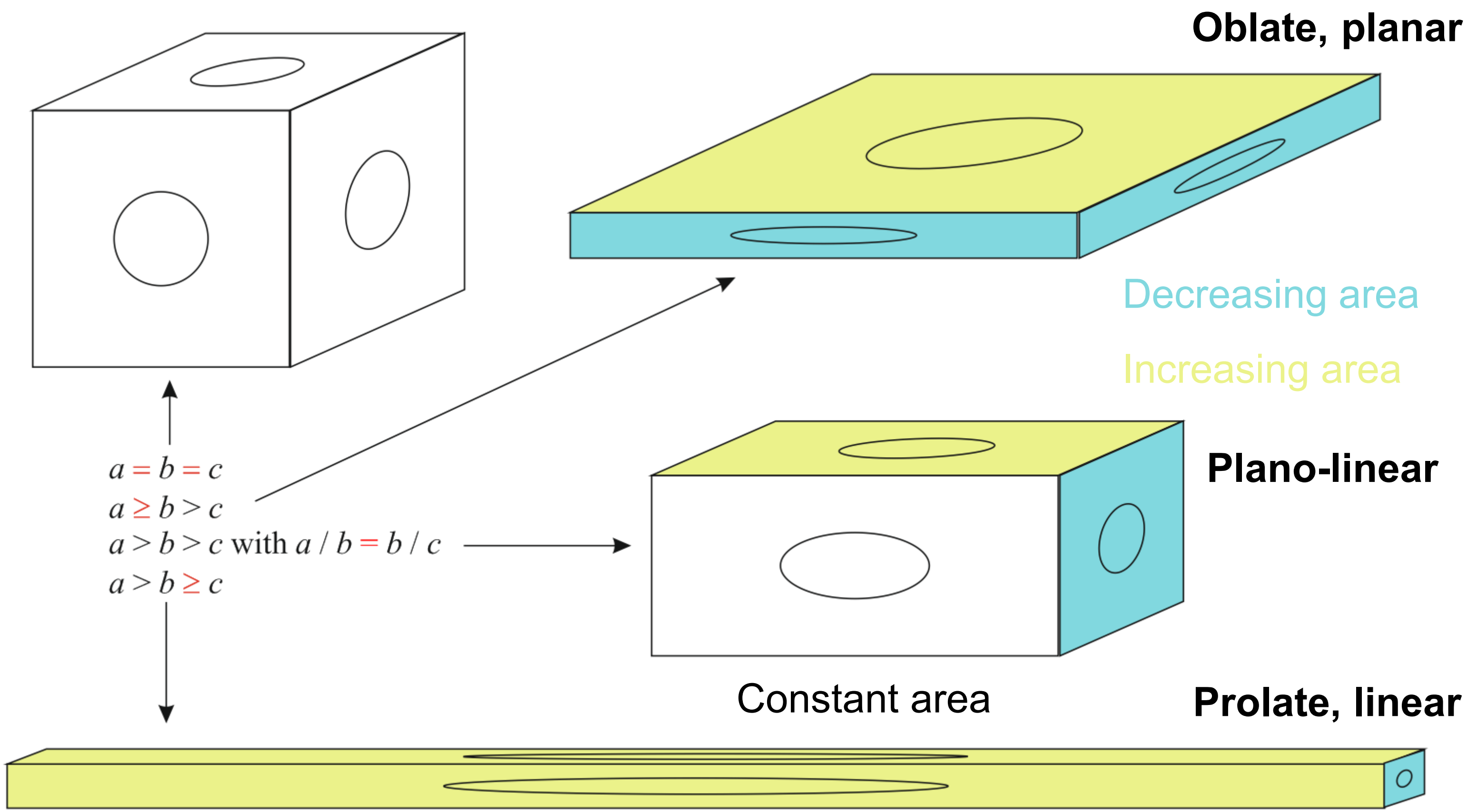

Prolate → linear, elongated, constrictive deformation
Planolinear → simple shear, uniaxial pure shear
Oblate → planar, flattened, divergent deformation

Normalization to an unitary volume: $a_n = l_1 / \sqrt[3]{\lambda_1 \cdot \lambda_2 \cdot \lambda_3}$

Let now considers 2 ellipses with individual shape ratio r forming an angle ω with the mean direction. 2 perpendicular ellipses would simulate an isotropic initial angular distribution with a resulting mean shape ratio R = 1 and PO Rf = 1 with ω = 45°.
A rotation of both ellipses as **rigid bodies** toward each other makes them parallel with $\omega = 0$, $R = r$ and Rf infinite.

$R \leq \sqrt{Rf}$ when $r \geq 10$

$R < \sqrt{Rf}$ when $1 < r < 10$

R=1,5 $\sqrt{Rf} = 1{,}7$

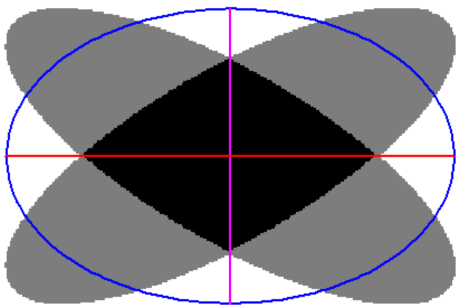

$\omega = 30°$

Mean SPO

R=3 $\sqrt{Rf} = \infty$

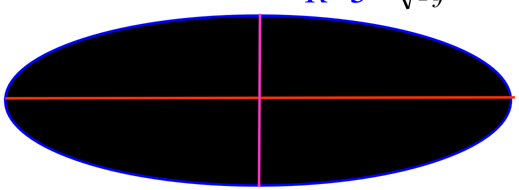

$\omega = 0°$

$\omega+\pi/2$

$$R = \frac{d(\omega)}{d(\omega+\pi/2)}$$

Normalization to k

$$K = \frac{R^2-1}{R^2+1} \quad k = \frac{r^2-1}{r^2+1}$$

$$K_n = K / k$$

$$R_n = \sqrt{\frac{1+K_n}{1-K_n}}$$

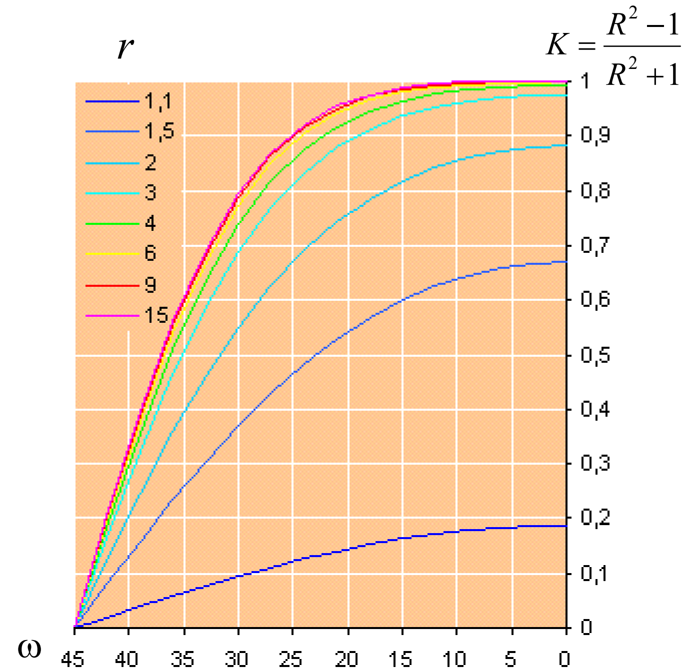

In such case a normalization to the shape parameter k can retrieve a PO R_n independent to the shape ratio r.

K: Willis (1977), Fernandez *et al*. (1983); K_n Launeau (2004)

A low contrast of viscosity produces the **passive deformation** of enclave in magma

An infinite contrast of viscosity between rigid crystals and its embedding viscous magma produces **active deformation** which is a free rotation of **rigid bodies** suspended in a flowing viscous matrix. In such case the crystals keep their shape and rotate progressively towards the shear plane forming crystal **shape preferred orientation** with an individual cyclicality proportional to their crystal shape ratio

Particle interactions
may slow down the
rigid body rotation

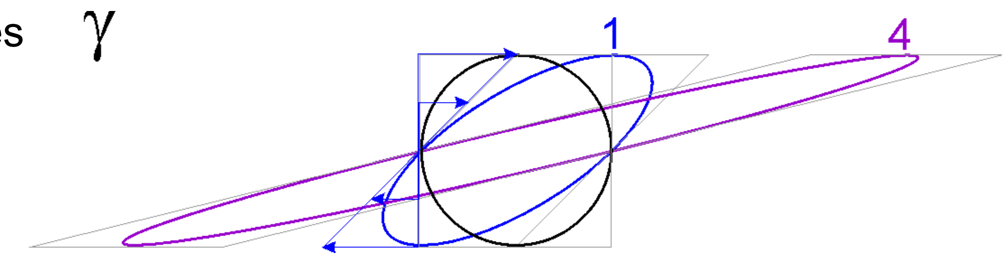

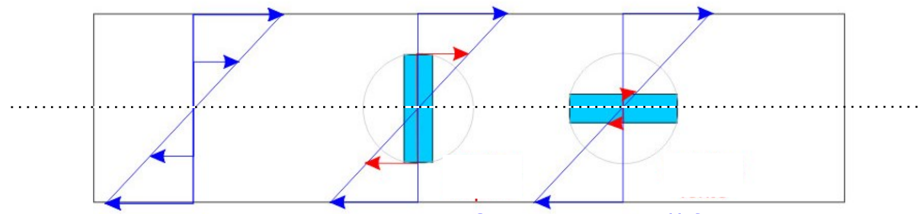

A rigid body can not deform, it turns on itself to allow the deformation of the magma

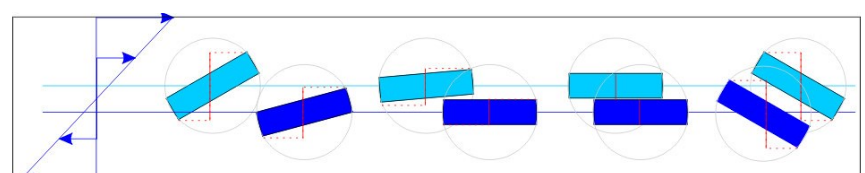

Launeau (2004)

Passive deformation of an enclave compared to

2D simulation of crystals **rigid body rotation** analyzed with the cosine direction method

2D simple shear equation of G.B. Jeffery (1922) giving the final orientation β' to the shear plane as a function of its initial orientation β, r and γ

$$\tan\beta' = r\cdot\tan\left[\frac{r\cdot\gamma}{r^2+1}+\arctan\left(\frac{\tan\beta}{r}\right)\right]$$

Rf is cyclic with $Rf_{max} = r^2$ at the critical γ_c (A. Fernandez *et al*. 1983)

$$\gamma_c = \frac{\pi}{\sqrt{1-k^2}} \qquad k = \frac{r^2-1}{r^2+1}$$

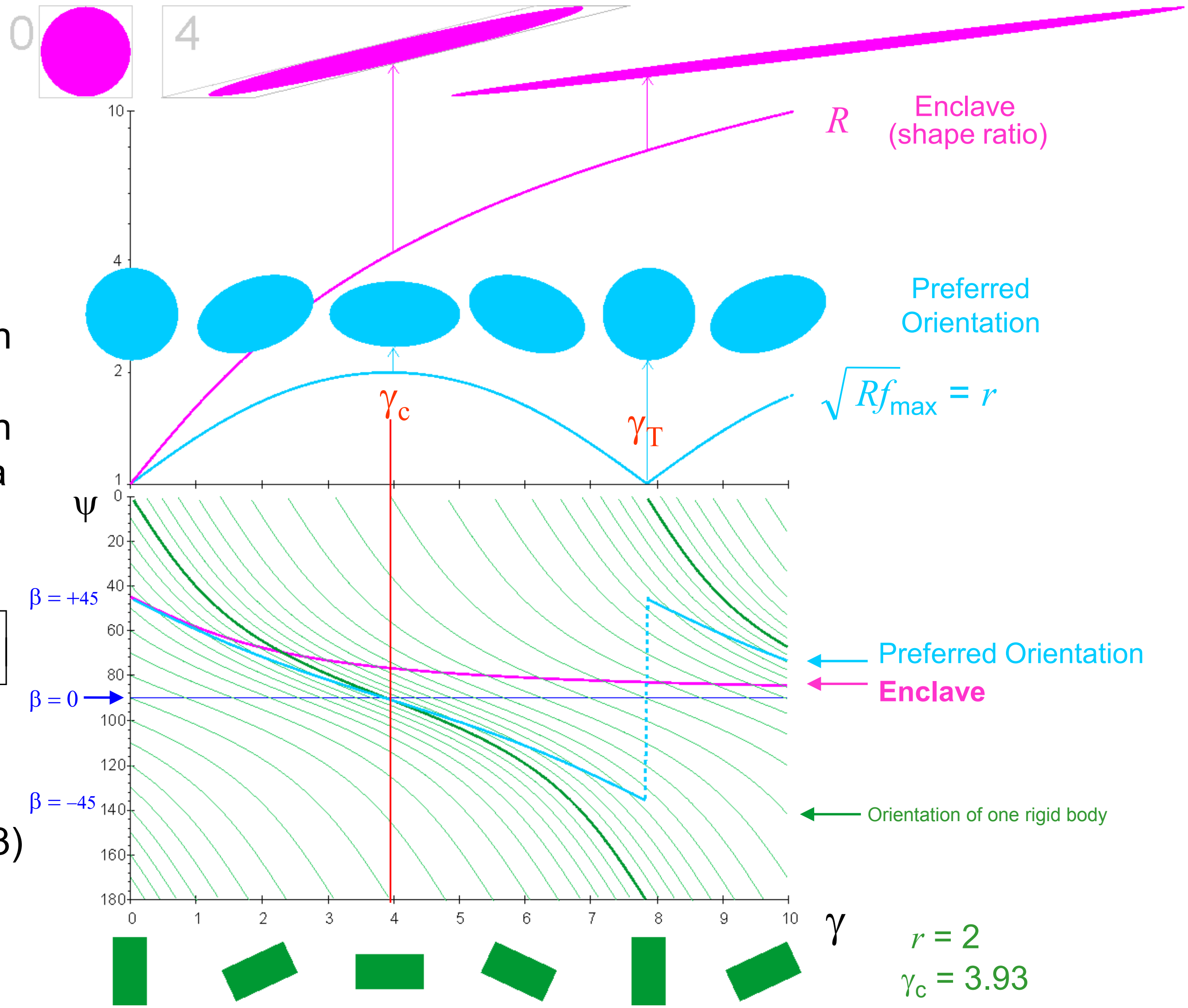

Launeau (2004)

3D simulation of rigid body rotation analyzed with the cosine direction method.

Equation of axisymmetric prolate boby ($a > b = c$)

The shape ratio $r = a/c$

Each body rotates faster at high angle with the shear plane and slows down along that shear plane

Jeffery (1922), Reed and Tryggvason (1974) et Willis (1977)

$$\tan\beta' = r \cdot \tan\left[\frac{r\cdot\gamma}{r^2+1} + \arctan\left(\frac{\tan\beta}{r}\right)\right] \qquad \tan^2\psi' = \tan^2\psi \cdot \left(\frac{r\cdot\cos^2\beta + \sin^2\beta}{r\cdot\cos^2\beta' + \sin^2\beta'}\right)$$

r = 1.5

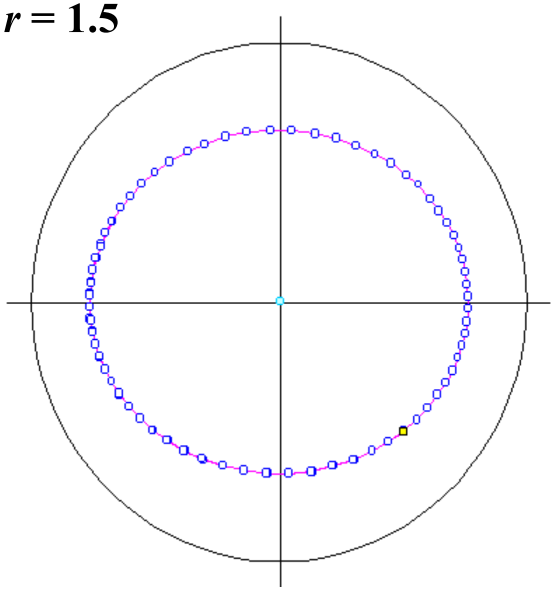

r = 2.5

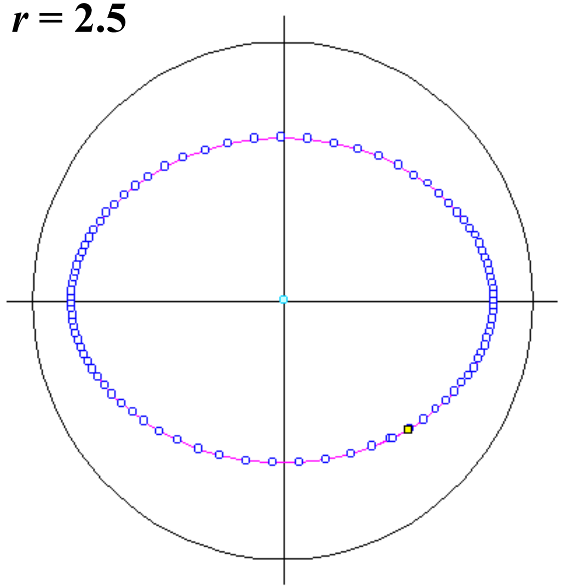

$a : b : c$ 1.5 : 1 : 1 2.5 : 1 : 1

Let build a population with random orientation and typical distribution of body shape ratio ranging from 1.15 to 3.4 with a mean shape ratio 2 and simulate a 3D shear flow.

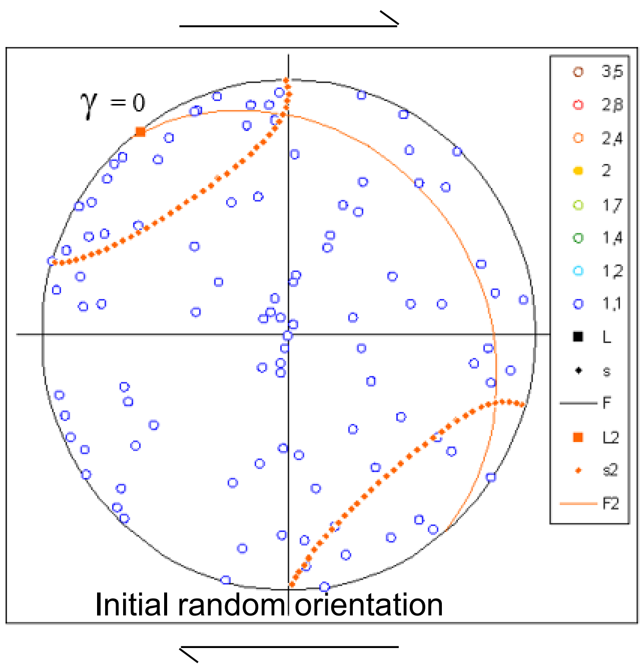

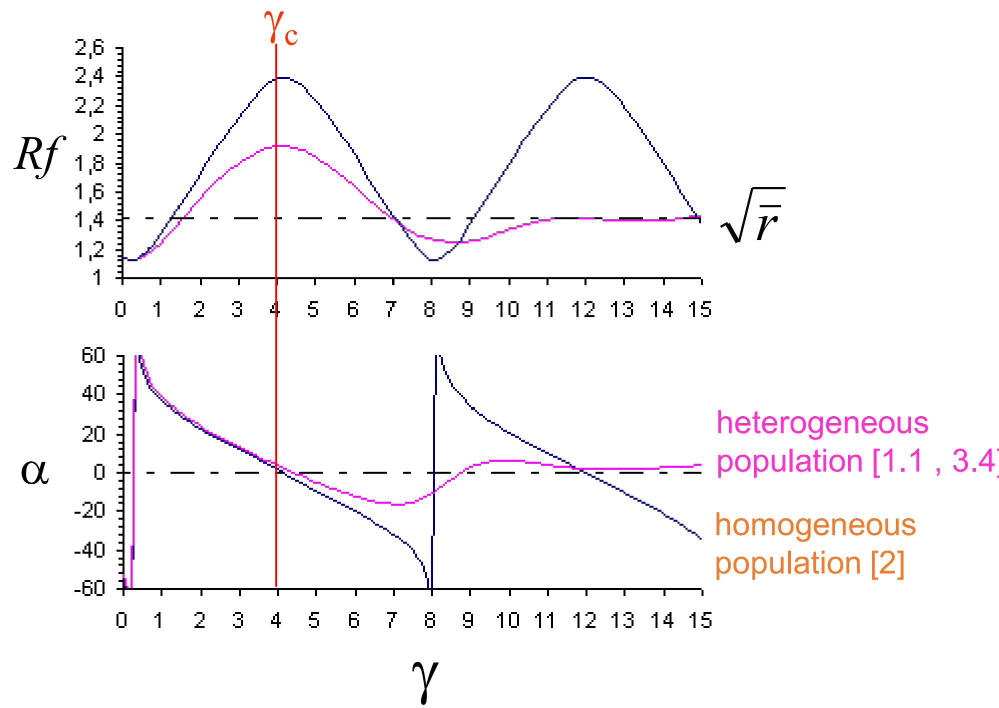

Mean Ellipsoid 2:1:1 $r_{a/c} = 2$ $\gamma_c = 3.93$

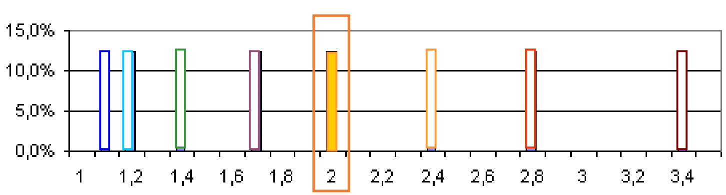

Each shape ratio sub population displays a perfect cyclic rotation whereas the accumulation of all populations quickly looses this cyclic rotation after γ_c and tend to become stable over the shear plane with a maximum $Rf_{max} = \sqrt{r}$

Launeau (2004)

The initial orientation does not matter either since strongly oblate and prolate orientation distributions of rigid bodies tend to stabilized themselves on the shear plane with increasing deformation.

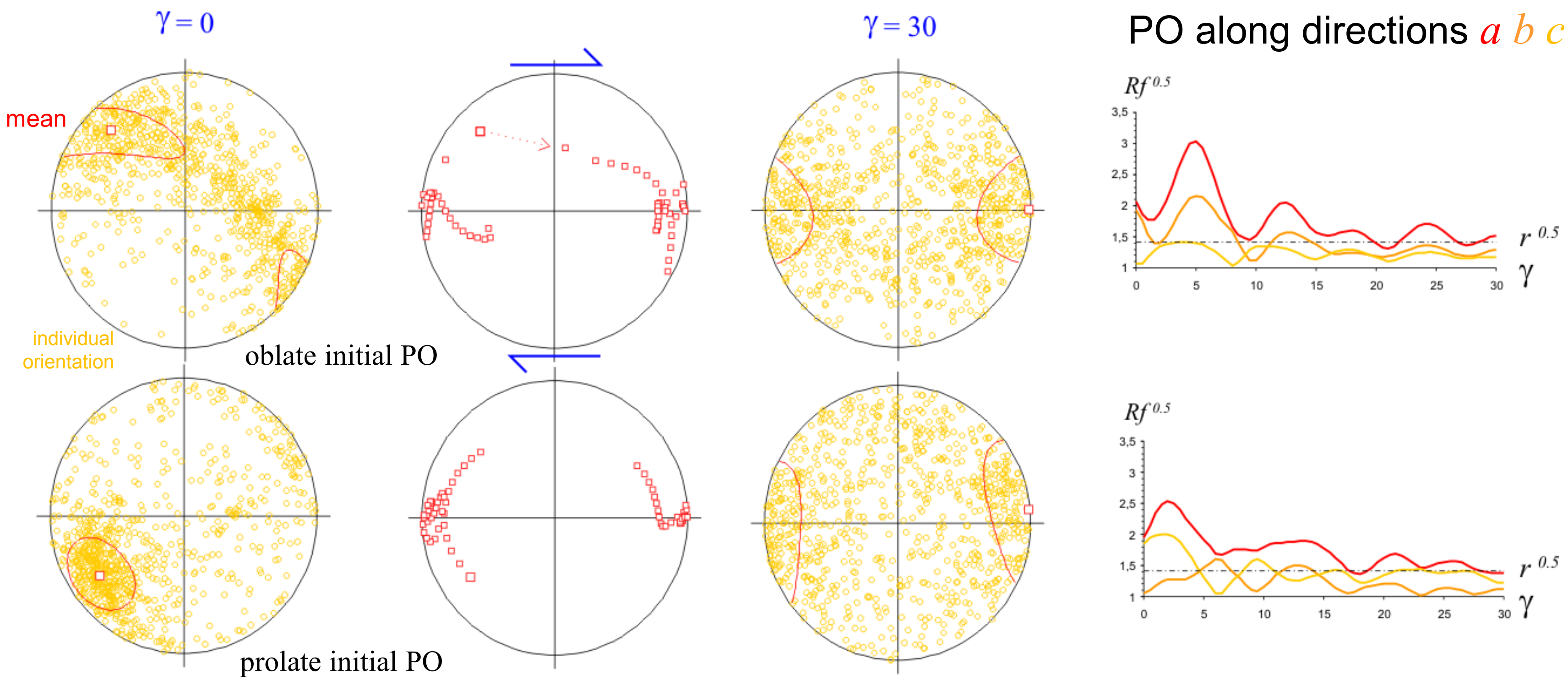

Mean Ellipsoid 2:1:1 $r_{a/c} = 2$ $\gamma_c = 3.93$

Launeau (2004)

To summarize, the passive deformation of a body with its matrix produces a mean shape proportional to the strain whereas the free rotation in the active deformation of rigid body produces a mean shape more or less aligned along the matrix shear plane

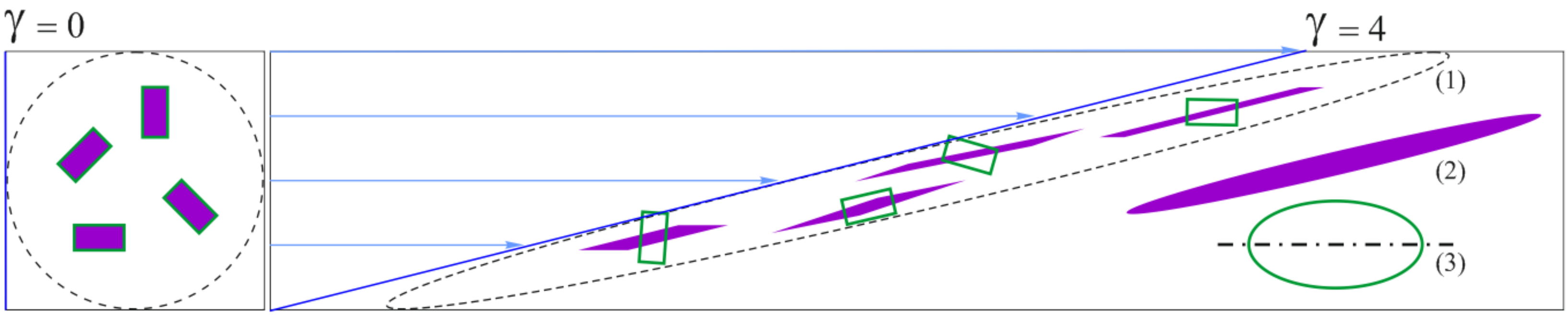

$r = 2 \quad \gamma_c = 3.93$

(1) Envelope of the magma bubble recording the strain
(2) Mean shape preferred orientation of passive bodies recording the strain
(3) Mean shape preferred orientation of rigid bodies converging towards the shear flow plane (// flow plane at γ_c)

The obliquity between passive elongation direction of an enclave and its internal crystal SPO potentially gives the shear sense of the magma flow

Launeau (2004)

Shape Preferred Orientation (OCW-UN-SPO) Launeau P. 2017

The shear flow is often stronger in contact with the floor and progressively decrease with the thickness of the magma toward the top of it where crystals and matrix are translated without internal magmatic deformation

Long translation with weak deformation

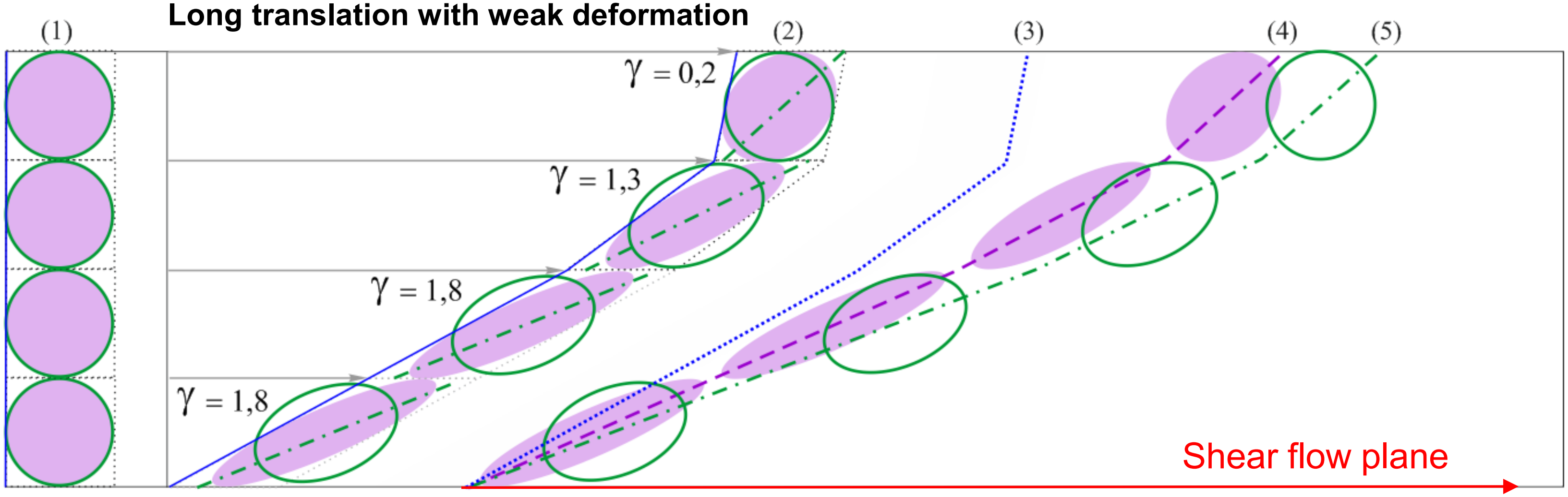

Short translation with strong deformation

(1) Initial position of a magma bubble
(2) Final position of its vertical section in blue, its shape in purple, the preferred orientation of its microlithes in green
(3) Alignment of the initial vertical sections of the magma bubbles
(4) Alignment of the ellipses of magma deformed passively obtained with translation indicating that its is virtual
(5) Alignment of the ellipses of crystal preferred orientation obtained with translation indicating that its is virtual (compare with (2))

All alignments are virtual and should not be confused with true flow planes, thus magmatic SPO lineations [A] and foliations (A,B) are indicators of (passive) flow strain or (active) flow pattern oblique on the effective flow plane.

Launeau (2004)

The degree of orientation can also be measured with *DO* as it follows

$$K_m = \frac{Rf - 1}{Rf + 1}$$

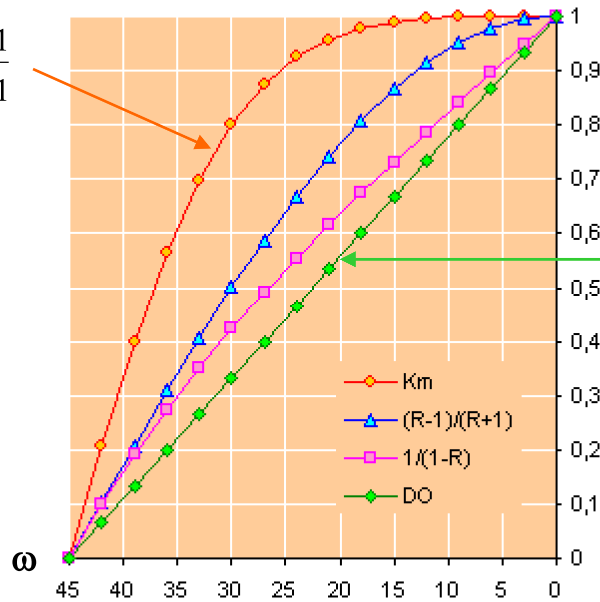

$$DO = 1 - \frac{4 \cdot \omega}{\pi} \qquad DO = 1 - \frac{4 \cdot \omega^\circ}{180^\circ}$$